

UNCLASSIFIED

AD 414681

DEFENSE DOCUMENTATION CENTER

FOR

SCIENTIFIC AND TECHNICAL INFORMATION

CAMERON STATION, ALEXANDRIA, VIRGINIA



UNCLASSIFIED

NOTICE: When government or other drawings, specifications or other data are used for any purpose other than in connection with a definitely related government procurement operation, the U. S. Government thereby incurs no responsibility, nor any obligation whatsoever; and the fact that the Government may have formulated, furnished, or in any way supplied the said drawings, specifications, or other data is not to be regarded by implication or otherwise as in any manner licensing the holder or any other person or corporation, or conveying any rights or permission to manufacture, use or sell any patented invention that may in any way be related thereto.

MEMORANDUM
RM-3792-PR
AUGUST 1963

CATALOGED BY DDC
AS AD NO. 414681

SIMILAR SOLUTIONS OF THE LAMINAR
BOUNDARY-LAYER EQUATIONS WITH
VARIABLE FLUID PROPERTIES

Joseph F. Gross and C. Forbes Dewey, Jr.

PREPARED FOR:
UNITED STATES AIR FORCE PROJECT RAND

The **RAND** *Corporation*
SANTA MONICA • CALIFORNIA

414681

MEMORANDUM

RM-3792-PR

AUGUST 1963

**SIMILAR SOLUTIONS OF THE LAMINAR
BOUNDARY-LAYER EQUATIONS WITH
VARIABLE FLUID PROPERTIES**

Joseph F. Gross and C. Forbes Dewey, Jr.

This research is sponsored by the United States Air Force under Project RAND—contract No. AF 49(638)-700 monitored by the Directorate of Development Planning, Deputy Chief of Staff, Research and Development, Hq USAF. Views or conclusions contained in this Memorandum should not be interpreted as representing the official opinion or policy of the United States Air Force.

PREFACE

The design of hypersonic vehicles has stimulated a large number of fluid-mechanical studies concerned with the hypersonic boundary layer. This Memorandum enlarges the scope of these studies to include various models for the fluid viscosity, the effect of high mass-injection rates at the stagnation point, and solutions at the hypersonic limit where the free-stream velocity is very high. These results should be useful as a guide in the design of vehicles operating at hypersonic speed.

This study is one of a series dealing with the hypersonic laminar boundary layer, and part of continuing RAND research in theoretical fluid mechanics.

SUMMARY

This Memorandum presents certain numerical solutions to the laminar boundary-layer similarity equations which illustrate the effects of Prandtl number, viscosity-temperature variation, mass transfer, wall temperature, pressure gradient, and hypersonic parameter σ on the structure of the boundary layer and the derivatives of velocity (shear force) and total enthalpy at the wall.

The results show that the common boundary-layer simplifications (such as Prandtl number = 1, viscosity proportional to temperature, zero pressure gradient) often lead to numerical errors of 20 to 50 per cent in the predicted heat transfer, skin friction, and displacement thickness. The shear and enthalpy gradient are shown to depend on the form of the viscosity-temperature relation, the Prandtl number, and the hypersonic parameter σ . Results for high surface mass-injection rates at the stagnation point indicate that the shear at the wall does not vanish as in the case of a flat plate.

ACKNOWLEDGMENT

The authors wish to express their appreciation to James I. Carlstedt for his able assistance in implementing the numerical techniques used in the solution of the boundary-layer equations.

CONTENTS

PREFACE	iii
SUMMARY	v
ACKNOWLEDGMENT	vii
LIST OF SYMBOLS	xi
LIST OF FIGURES	xiii
Section	
I. INTRODUCTION	1
II. THE SIMILARITY EQUATIONS	3
III. EFFECTS OF THE TEMPERATURE-VISCOSITY LAW	5
Velocity and Enthalpy Profiles with a Power-Law	
Viscosity	6
Effects of Viscosity Law on Skin Friction and Heat	
Transfer	6
Relation Between Sutherland and Power-Law	
Viscosity Functions	12
IV. EFFECTS OF THE PRANDTL NUMBER	16
V. EFFECTS OF LARGE INJECTION	20
VI. BEHAVIOR OF THE BOUNDARY LAYER IN THE HYPERSONIC LIMIT.	25
VII. CONCLUDING REMARKS	28
REFERENCES	31

LIST OF SYMBOLS

- C^* = Chapman-Rubesin constant, $\rho\mu/\rho_e\mu_e$
- c_f = skin-friction coefficient
- c_p = specific heat
- f' = transformed velocity function, u/u_e
- H = total enthalpy, $c_p T + 1/2 (u^2 + v^2)$
- I_1 = transformed displacement thickness, $\int_0^{\infty} f'(1 - f') d\eta$
- k = thermal conductivity
- Pr = Prandtl number, $c_p\mu/k$
- Re_x = Reynolds number based on free-stream properties, $\rho u x/\mu$
- T = temperature
- T_0 = stagnation temperature
- T_r = reference temperature (Eq. (11))
- t = normalized temperature, T/T_0
- u, v = velocity components in the x, y directions, respectively
- x, y = axial and normal surface coordinates, respectively
- β = pressure-gradient parameter (Eq. (5))
- γ = ratio of specific heats, c_p/c_v
- η, ξ = similarity variables (Eqs. (6) and (7))
- θ = dimensionless total enthalpy, $(H - H_w)/(H_e - H_w)$
- μ = dynamic viscosity
- ρ = density

σ = hypersonic parameter, $(u_\infty^2/2H_e)(u_e^2/u_\infty^2)$

ω = exponent in temperature-viscosity relation $\mu \sim T^\omega$

Subscripts and Superscripts

aw = evaluated for $\theta'_w = 0$

e = evaluated at the edge of the boundary layer

r = evaluated at the reference temperature T_r

w = evaluated at the wall

∞ = evaluated in the free stream

' = derivative with respect to η

o = evaluated at the stagnation temperature T_o

LIST OF FIGURES

1. Velocity and enthalpy distributions across the laminar boundary layer: $\beta = 0, \sigma = 1$	7
2. Velocity and enthalpy distributions across the laminar boundary layer: $\beta = 0.5, \sigma = 0$	8
3. Effects of Sutherland constant on heat transfer	9
4. Effects of power-law exponent on heat transfer	9
5. Effects of wall temperature on heat transfer	11
6. Effects of pressure gradient on skin friction	11
7. Wall velocity-gradient differences between the two viscosity laws	14
8. Variation of ω_r with Sutherland constant and wall temperature	15
9. Velocity and enthalpy distributions for different Prandtl numbers	17
10. Effects of Prandtl number on heat transfer	18
11. Wall velocity gradient and heat transfer with large injection: two-dimensional stagnation point	21
12. Velocity and velocity-gradient distributions with injection	23
13. Enthalpy and enthalpy-gradient distributions with injection	24
14. Influence of hypersonic parameter σ on skin friction, heat transfer, and displacement thickness: $t_w = 0.15$	26
15. Influence of hypersonic parameter σ on skin friction, heat transfer, and displacement thickness: $t_w = 0.60$	26

I. INTRODUCTION

In most physical situations, the laminar boundary layer which develops along the surface of a body in high-speed flow does not behave in an exactly similar manner. That is, the mathematical restrictions necessary to reduce the partial differential equations governing boundary-layer motion to ordinary differential equations in transformed coordinates are not exactly satisfied. Of the several concepts which have been proposed to deal with such circumstances, local similarity is perhaps the most successful. The local similarity concept assumes that at every streamwise station the boundary layer adjusts to changes in the geometric and thermodynamic boundary conditions and is identical in all essential respects to the similar-solution boundary layer whose history includes the local boundary conditions.

In this context, similar solutions to the laminar boundary-layer equations are of great utility in predicting the skin friction, heat transfer, and boundary-layer displacement thickness for a wide variety of "smooth" body shapes. A large number of solutions to the low-speed and stagnation-point boundary-layer problems have been published, but little systematic work has been done on the important effects of viscous dissipation with $Pr \neq 1$ and variations of the $(\rho\mu)$ product with temperature. The lack of adequate solutions is particularly evident in the hypersonic limit, $\sigma \equiv (u_\infty^2/2H_e)(u_e/u_\infty)^2 \rightarrow 1$.*

This Memorandum presents selected numerical solutions to the laminar boundary-layer similarity equations which illustrate systematically the effects of Prandtl number, viscosity-temperature variation, mass transfer, wall temperature, pressure gradient, and hypersonic parameter σ on the structure of the boundary layer and the derivatives of velocity and total enthalpy at the wall. It will be found that the common boundary-layer simplifications (such as $Pr = 1$, $\rho\mu = \text{constant}$, or $\beta = 0$) often lead to numerical errors of 20 to 50 per cent in the predicted heat transfer, skin friction, and displacement thickness.

*The quantity σ will be referred to as the "hypersonic parameter," and $\sigma \rightarrow 1$ will be called the "hypersonic limit."

Furthermore, the shear and enthalpy-gradient profiles in the boundary layer depend strongly on the assumed form of the viscosity-temperature relation and the Prandtl number, and also on the hypersonic parameter σ .

II. THE SIMILARITY EQUATIONS

The partial differential equations governing the two-dimensional compressible laminar boundary layer in a perfect gas may be reduced to the following pair of coupled ordinary differential equations; ^{(1)*}

$$\frac{d}{d\eta} \left(\frac{\rho\mu}{\rho_w\mu_w} f'' \right) + ff'' - \beta \left[f'^2 - (1 - t_w) \theta - t_w \right] = 0 \quad (1)$$

$$\frac{d}{d\eta} \left(\frac{1}{Pr} \frac{\rho\mu}{\rho_w\mu_w} \theta' \right) + f\theta' + \frac{d}{d\eta} \left[\left(1 - \frac{1}{Pr} \right) \left(\frac{\rho\mu}{\rho_w\mu_w} \right) \frac{2\sigma f'^2}{(1 - t_w)} \right] = 0. \quad (2)$$

The boundary conditions are written

$$\eta = 0 \quad f' = \theta = 0; f = f_w = \text{constant} \quad (3)$$

$$\eta \rightarrow \infty \quad f' = \theta = 1, \quad (4)$$

where f' is the normalized velocity (u/u_e), θ is the normalized total enthalpy $(H - H_w)/(H_e - H_w)$, and σ is the hypersonic parameter $(u_\infty^2/2H_e)(u_e/u_\infty)^2$. The derivation leading to Eqs. (1) and (2) assumes that both the specific heat c_p and the pressure-gradient parameter β are constant; β is defined by the equation

$$\beta = - \frac{\gamma - 1}{\gamma} \frac{\int_0^x \rho_w \mu_w u_e dx}{\rho_w \mu_w u_e x} \frac{x}{p_e} \frac{dp_e}{dx}. \quad (5)$$

*The effects of sweep may also be studied in a similar manner; this increases the number of coupled equations to three, and analogous results may be obtained. The effects of sweep may be found in Refs. 1 and 2.

The similarity variable η is defined by

$$\eta(x, y) = \frac{u_e}{(2\xi)^{1/2}} \int_0^y \rho \, dy, \quad (6)$$

where

$$\xi(x) = \int_0^x \rho_w \mu_w u_e \, dx. \quad (7)$$

Equations (1) - (4) have been solved using standard numerical-integration techniques. An extensive tabulation of solutions is presently being prepared by the authors. The typical results reported in this Memorandum were selected to illustrate the most important conclusions derived from these solutions. Empirical techniques for estimating effective fluid-property variations across the boundary layer are also suggested.

The physical significance of the hypersonic parameter can be seen by noting its structure and position in the energy equation. In Eq. (2), it is clear that for $Pr = 1$, the viscous-dissipation term containing σ vanishes. For $Pr \neq 1$, the value of σ determines to some degree the role of the viscous-dissipation term in the energy equation. The hypersonic parameter σ is composed of two terms, $(u_\infty^2/2H_e)$ and $(u_e/u_\infty)^2$. At the stagnation point, $(u_e/u_\infty)^2 = 0$; on the other hand high-speed boundary layers are characterized by $(u_e/u_\infty)^2 \sim 1$ if the free-stream velocity is high, that is, $(u_\infty^2/2H_e) \rightarrow 1$.

III. EFFECTS OF THE TEMPERATURE-VISCOSITY LAW

Equations (1) and (2) are greatly simplified if the product $(\rho\mu)$ is constant across the boundary layer. Since $p = p(x)$ only in the boundary-layer approximation, this requires $\mu \sim T^\omega$ with $\omega = 1$. It has been shown by several authors (e.g., Van Driest⁽³⁾) that the form of the viscosity-temperature relation plays an important role in determining the properties of the boundary layer.

Two alternative forms of $\mu(T)$ have been proposed. These are the power-law representation

$$\mu \sim T^\omega, \quad \frac{1}{2} \leq \omega \leq 1 \quad (8)$$

and the Sutherland formula

$$\frac{\mu}{\mu_0} = (t)^{3/2} \left[\frac{s+1}{s+t} \right], \quad 0 \leq s, \quad (9)$$

where s and ω are parametric constants, and $t = (T/T_0)$.

In view of the fact that Sutherland's law represents an approximation to the intermolecular potential, the power-law variation of viscosity appears to be equally suitable as a one-parameter representation of the viscosity-temperature law, and it offers certain conceptual advantages when dealing with air and other gases at high temperature. The power-law representation, however, provides a less accurate representation of the function $\mu(T)$ over an extended range of temperature.

Two related problems will be considered with respect to the function $\mu(T)$. First, we wish to examine the effects of the temperature-viscosity parameters ω and s on the velocity and enthalpy profiles within the boundary layer. And second, we wish to demonstrate that the two parametric forms of the viscosity-temperature law are equivalent, and that they are simply related through the concept of a reference temperature.

VELOCITY AND ENTHALPY PROFILES WITH A POWER-LAW VISCOSITY

The effects of changing the exponent in the power-law expression for the viscosity are shown in Figs. 1 and 2. A value $\omega = 0.7$ corresponds closely to conventional wind-tunnel conditions, while $\omega = 0.5$ represents conditions encountered in hypersonic flight. The value $\omega = 1$ represents the simplification $(\rho\mu) = \text{constant}$ which has been widely used in studying the laminar boundary layer. The values $\beta = 0.5$ and $\sigma = 0$ are appropriate to axisymmetric stagnation-point flow, while $\beta = 0$ and $\sigma = 1$ represent the hypersonic laminar boundary layer over a flat plate.

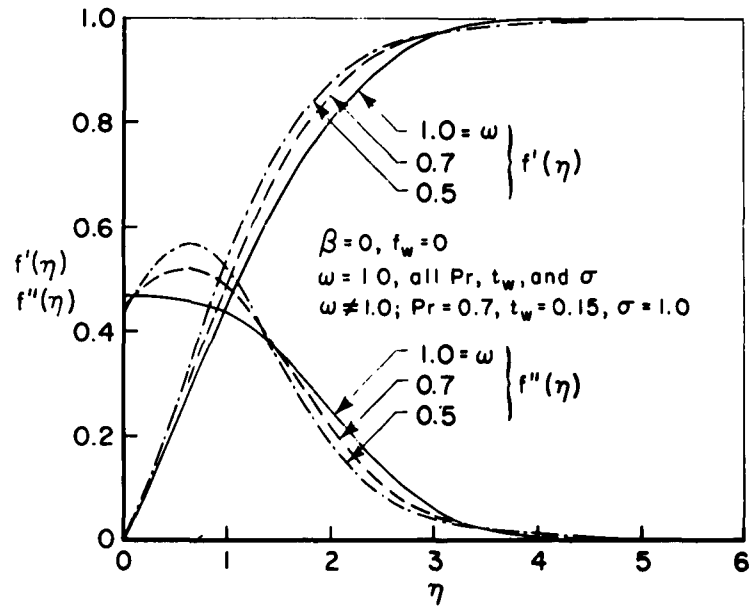
Several important effects may be discerned in Figs. 1 and 2. First, decreasing values of ω decrease the 0.90 thicknesses* of the velocity and total-enthalpy boundary layers. Second, the variable viscosity introduces a distinct inflection in the velocity and enthalpy profiles, as evidenced by a maximum in the derivatives $f'(\eta)$ and $\theta'(\eta)$. Since the existence of an inflection point in the velocity profile is related to the stability of the laminar boundary layer, this effect may explain the anomalous result of stability theories based on $\omega = 1$ that the critical transition Reynolds number for a flat plate becomes infinite with a highly cooled wall. The fact that the wall derivatives f'_w and θ'_w for $\beta = 0$ are nearly independent of the value of ω appears to be fortuitous. The variations of f' , f'' , θ , and θ' with ω are considerably reduced at higher values of the wall temperature t_w .

EFFECTS OF VISCOSITY LAW ON SKIN FRICTION AND HEAT TRANSFER

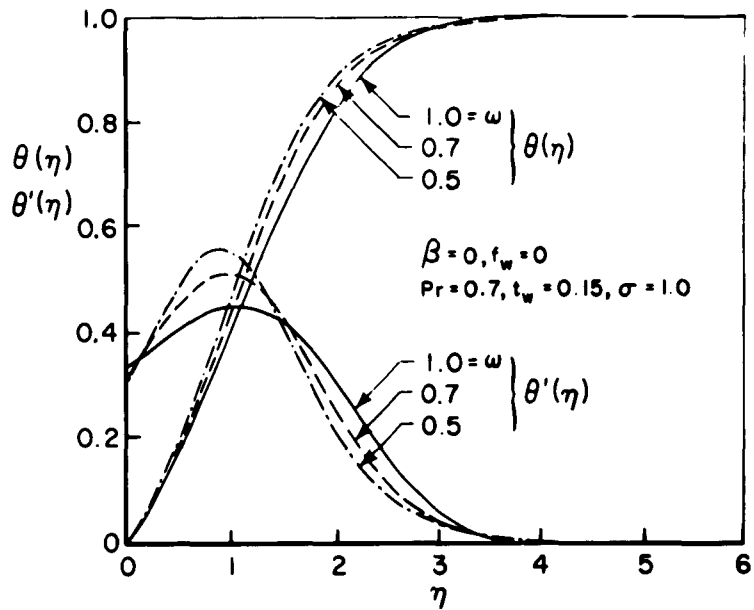
One of the purposes of this study is to examine the use of the Sutherland viscosity law in determining the properties of the hypersonic laminar boundary layer. In Fig. 3, the effects of pressure gradient, wall temperature, and the Sutherland constant s on the normalized heat transfer $\bar{\theta}'_w$ are shown. The normalized heat transfer $\bar{\theta}'_w$ is defined by

$$\bar{\theta}'_w = \theta'_w \frac{(1 - t_w)}{(t_{aw} - t_w)}, \quad (10)$$

*The points where the velocity and total enthalpy reach 0.90 of their values outside the boundary layer.

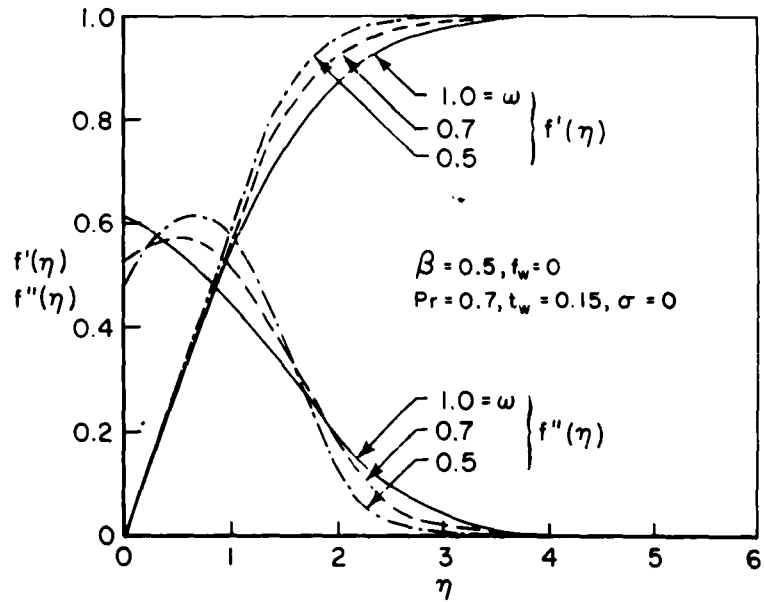


(a) Velocity and shear distributions

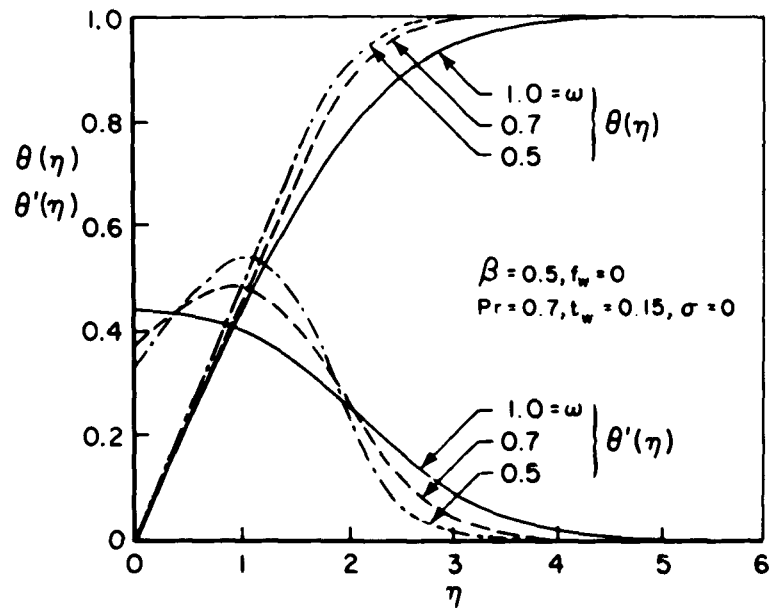


(b) Enthalpy and enthalpy-gradient distributions

Fig. 1---Velocity and enthalpy distributions across the laminar boundary layer: $\beta = 0, \sigma = 1$



(a) Velocity and shear distributions



(b) Enthalpy and enthalpy-gradient distributions

Fig. 2---Velocity and enthalpy distributions across the laminar boundary layer: $\beta = 0.5, \sigma = 0$

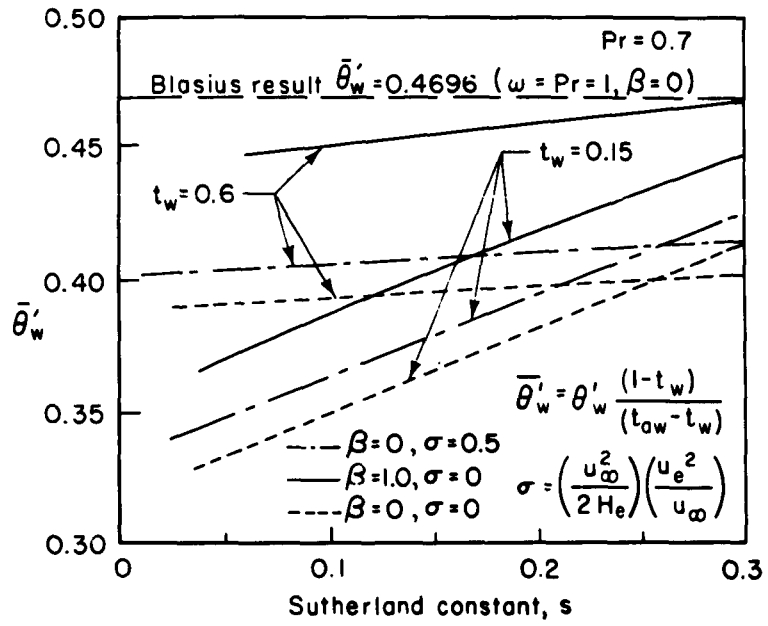


Fig. 3---Effects of Sutherland constant on heat transfer

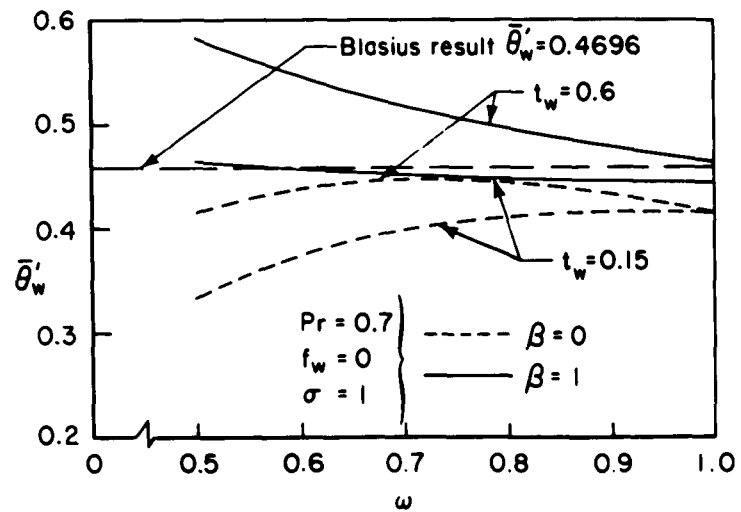


Fig. 4---Effects of power-law exponent on heat transfer

where

t_{aw} = adiabatic wall temperature

t_w = wall temperature

θ'_w = total enthalpy gradient at the wall.

The Blasius result ($\beta = 0$, $Pr = 1$, $\rho\mu = \text{constant}$) is given for comparison. The Sutherland constant s is defined by

$$s = \frac{S}{T_o}, \quad (11)$$

where S is a reference temperature for the particular gas under consideration. The constant $s \approx 0.2$ for ordinary wind-tunnel conditions, and $s \approx 0.02$ for hypersonic flight conditions.

The pressure-gradient effect is as expected. If the wall temperature and Sutherland constant are the same, then an increase of the pressure gradient increases the heat transfer at the wall. The dependence of the heat transfer on the Sutherland constant increases as the wall temperature decreases. At a value of $t_w = 0.6$, the normalized heat transfer $\bar{\theta}'_w$ is essentially independent of s . If the wall temperature is reduced to $t_w = 0.15$, then $\bar{\theta}'_w$ depends strongly on s ; the normalized heat transfer $\bar{\theta}'_w$ increases with increasing s .

Figure 4 shows the variation of the normalized heat transfer $\bar{\theta}'_w$ as a function of the power-law exponent ω for the hypersonic limit $\sigma = 1$. Here again, an increase in the pressure gradient or the wall temperature results in an increase in the normalized heat transfer. The values of $\bar{\theta}''_w$ seem to be more sensitive to the pressure gradient in the hypersonic limit $\sigma = 1$ and, in addition, are somewhat higher than they are at $\sigma = 0.5$. In general, the maximum variation of $\bar{\theta}''_w$ at a given wall temperature and pressure gradient with ω or s is less than 30 per cent.

Figures 5 and 6 are included to illustrate the magnitude of the effects of the viscosity-temperature relation on skin friction and heat transfer. In Fig. 5, the normalized heat transfer $\bar{\theta}'_w$ is shown as a function of t_w and ω . It is interesting to note that the single

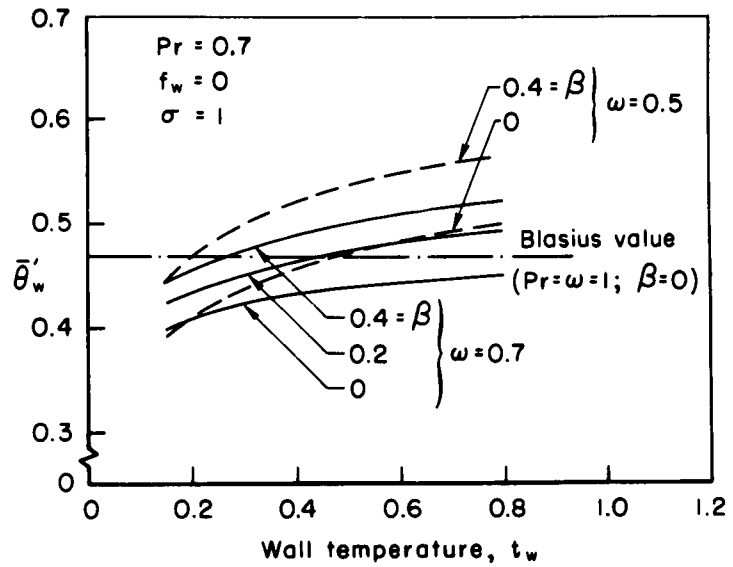


Fig. 5---Effects of wall temperature on heat transfer

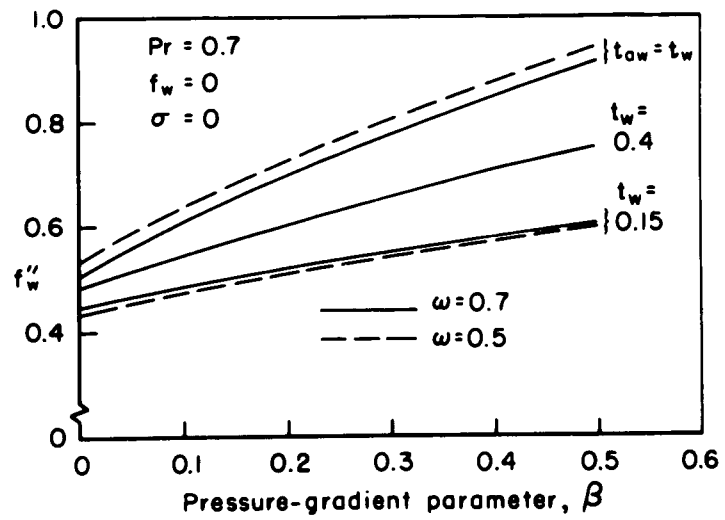


Fig. 6---Effects of pressure gradient on skin friction

Blasius value $\bar{\theta}'_w = 0.4696$ for $Pr = \omega = 1$ and $\beta = 0$ is a fortuitously good approximation to the exact value of $\bar{\theta}'_w$ over a large range of conditions. For any particular choice of conditions, however, such a simple approximation may be in error by as much as 30 per cent. The changes in $\bar{\theta}'_w$ introduced by variation of the exponent ω are of the same order as those introduced by the pressure-gradient parameter β and the wall temperature t_w . It is important, therefore, that a proper viscosity formulation be used when exact solutions are desired.

The wall velocity gradient f''_w is strongly affected by pressure gradient, as shown in Fig. 6. This is because the parameter β appears explicitly in the momentum equation (1); the effects of pressure gradient appear in the energy equation (2) only indirectly through the velocity ratio $f' = (u/u_e)$. It may be seen in Fig. 6 that the effects of the viscosity exponent on f''_w are small compared to the effects introduced by the pressure-gradient parameter. The effects of large values of β on the wall shear f''_w have been studied extensively by Cohen and Reshotko⁽⁴⁾ and others.

RELATION BETWEEN SUTHERLAND AND POWER-LAW VISCOSITY FUNCTIONS

Another purpose of the Sutherland-law investigation was to determine the relations between solutions obtained using a Sutherland-law viscosity and those obtained by the use of a power-law $\mu \sim T^{\omega}$ employing an empirically calculated ω_r .^{*} Solutions for specific boundary conditions were obtained using the Sutherland-law viscosity relationship. A reference temperature, t_r , was then used which was originally suggested by Rubesin and Johnson⁽⁵⁾ and modified by Eckert⁽⁶⁾ to provide an approximation method of evaluating the wall conditions for a compressible boundary layer. The Eckert reference temperature is given by

$$t_r = 0.5 (t_e + t_w) + 0.22 (1 - t_w) \quad (12)$$

^{*}It should be emphasized that the Sutherland law itself is derived from an empirical approximation to the intermolecular potential.

and was used to calculate an empirical ω_r from the following formula:

$$\omega_r = \frac{3}{2} + \frac{\ln\left(\frac{t_w + s}{t_r + s}\right)}{\ln\left(\frac{t_r}{t_w}\right)}. \quad (13)$$

An exact solution to the similar equations was then obtained using the temperature-viscosity relation $\mu \sim T^{\omega_r}$, and these results were compared with solutions obtained using the Sutherland law. Figure 7 shows the differences in the wall derivative f''_w obtained for some typical cases. Specifically, the graph shows $\Delta f''_w = f''_w(s) - f''_w(\omega_r)$ plotted as a function of s for different wall temperatures and pressure gradients. The maximum error is approximately 2.5 per cent in the wall velocity gradient; in most cases, the error is well below 1 per cent. Figure 7 also shows the effects of the important parameters t_w and β on the differences $\Delta f''_w$ induced by the use of the ω_r calculation. Clearly, the differences increase as s increases, and both the difference function and s must go to zero together (ω_r is identically 1/2 for $s = 0$). For the cold wall, the difference is greater because the power-law approximation cannot fit the Sutherland-law viscosity throughout the larger temperature range. These differences are reduced to negligible values for $t_w \geq 0.6$. The effect of pressure gradient at low wall temperature is also evident: An increase in β gives rise to an increase in the difference function $\Delta f''_w$. The higher pressure gradient causes the power-law approximation to be a less accurate fit of the Sutherland law. In general, the differences are quite small even for the cold-wall cases, and the power-law approximation using the Eckert reference temperature should prove to be a valuable empirical method.

The values of ω_r as a function of the Sutherland constant s are shown in Fig. 8 for the three wall temperatures $t_w = 0.15$, $t_w = 0.4$, and $t_w = 0.6$.

It can be seen that the empirically determined ω_r is a smooth function of the Sutherland constant s , so it will be possible to interpolate for conditions not presented in this Memorandum. When

$s \rightarrow 0, \omega_r \rightarrow 0.5$ for all values of t_w and t_e . The expression for ω_r also shows that increasing the wall temperature reduces the range of ω_r .

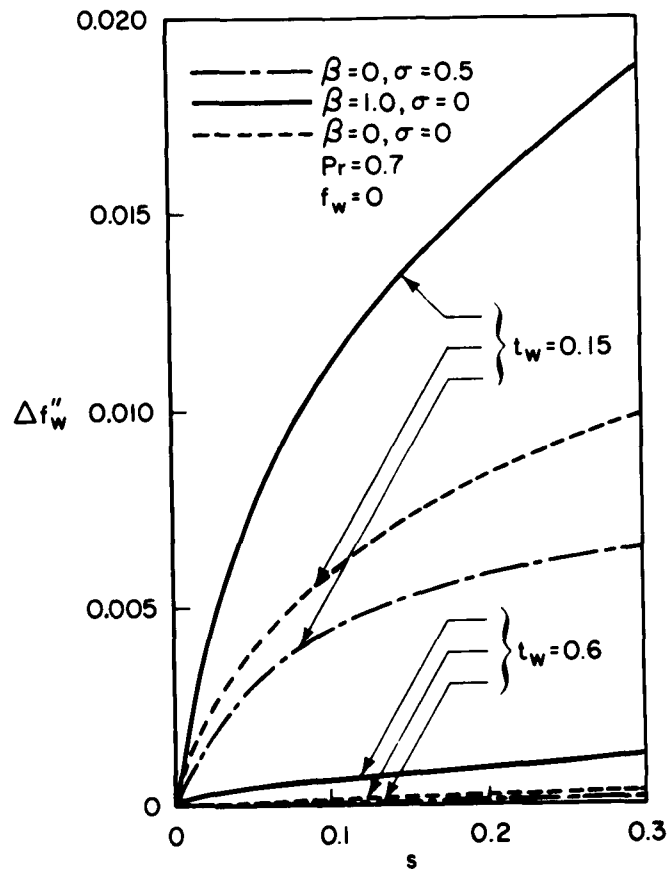


Fig. 7---Wall velocity-gradient differences between the two viscosity laws

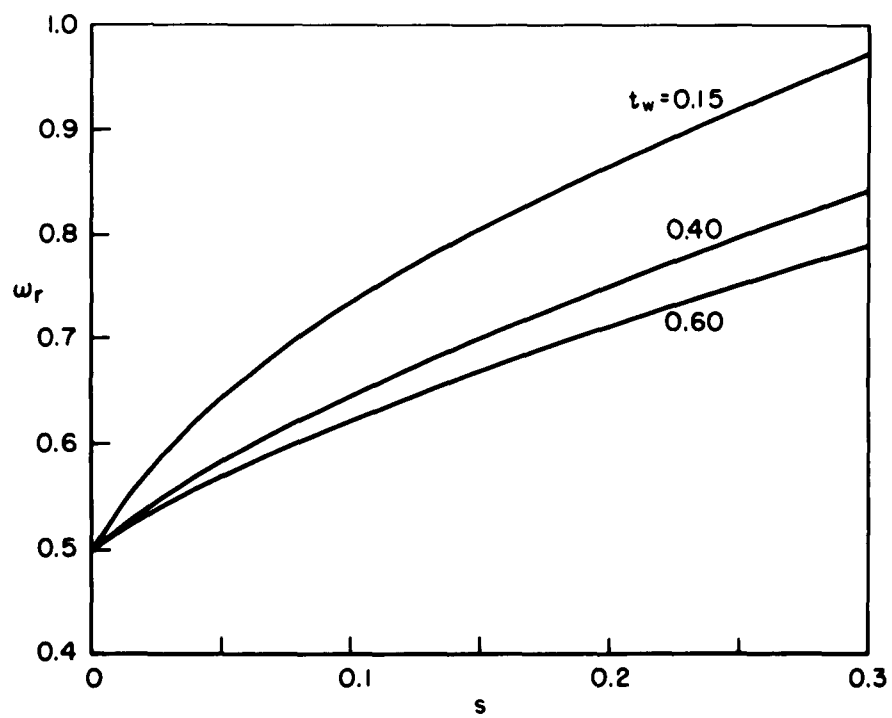


Fig. 8---Variation of ω_r with Sutherland constant and wall temperature

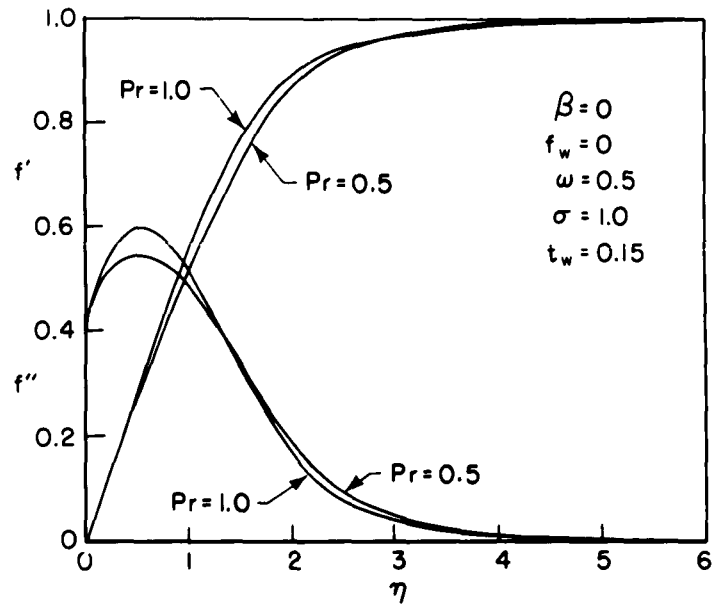
IV. EFFECTS OF THE PRANDTL NUMBER

The effects of the Prandtl number on the enthalpy and velocity distributions in the boundary layer are shown in Fig. 9 for the cold-wall case ($t_w = 0.15$) in the hypersonic limit, $\sigma = 1$. The velocity profiles are not noticeably affected, but there is a drastic change in the enthalpy gradient as well as the enthalpy distribution within the boundary layer. The wall enthalpy gradient is considerably reduced when the Prandtl number is decreased from 1.0 to 0.5. The enthalpy profile is less full for the $Pr = 0.5$ case, and this has the effect of concentrating the high enthalpy gradients near the outer edge of the boundary layer.

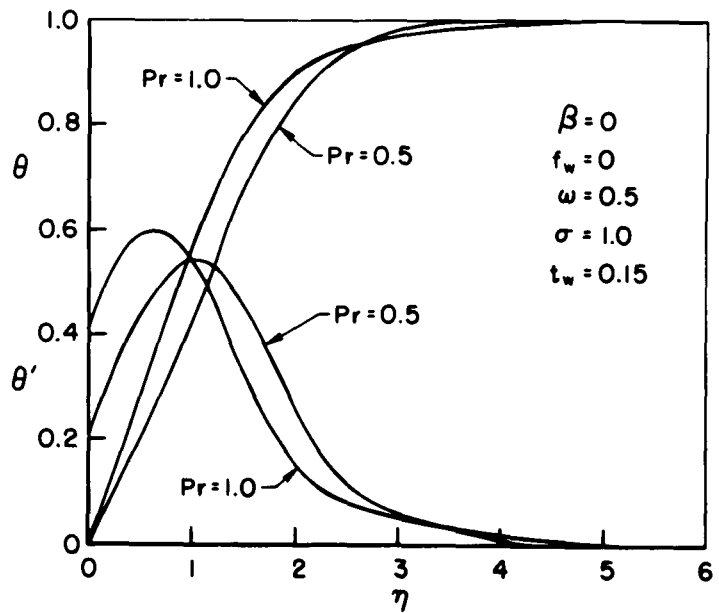
In order to demonstrate the effects of the Prandtl number more decisively, the wall enthalpy gradient θ'_w and the normalized heat-transfer parameter $\bar{\theta}'_w$ are plotted as functions of Pr in Fig. 10. It is shown in (a) of Fig. 10 that θ'_w increases with increasing Pr ; here, $\sigma = 0$, so that the dissipation term appearing in the energy equation (2) is identically zero. It may be seen that the common assumption of $Pr = 1$ for air introduces an error in θ'_w which is of the same order of magnitude (about 5 - 15 per cent) as the change in θ'_w due to a variation of the pressure-gradient parameter β from 0 to 0.5. It is therefore numerically inconsistent (at least for $\sigma = 0$) to include the effects of pressure gradient while neglecting the effects of Prandtl number.

In the hypersonic limit, $\sigma = 1$, the situation changes dramatically; (b) of Fig. 10 indicates the variation of θ'_w with Prandtl number for $\beta = 0$ with and without the viscous-dissipation term. The effects of Pr and wall temperature, t_w , on θ'_w are greatly increased by including the viscous-dissipation term. This is primarily because of the large change in the adiabatic wall temperature t_{aw} with Prandtl number. A useful empirical formula which relates the adiabatic wall temperature t_{aw} to the parameters Pr , ω , σ , β , and f_w is

$$t_{aw} = 1 + 1.428 \sigma (\sqrt{Pr} - 1) (1 + 0.29\beta) (1 - 0.3\omega) (1 - 0.95f_w). \quad (14)$$



(a) Velocity and velocity-gradient distributions



(b) Enthalpy and enthalpy-gradient distributions

Fig. 9---Velocity and enthalpy distributions for different Prandtl numbers

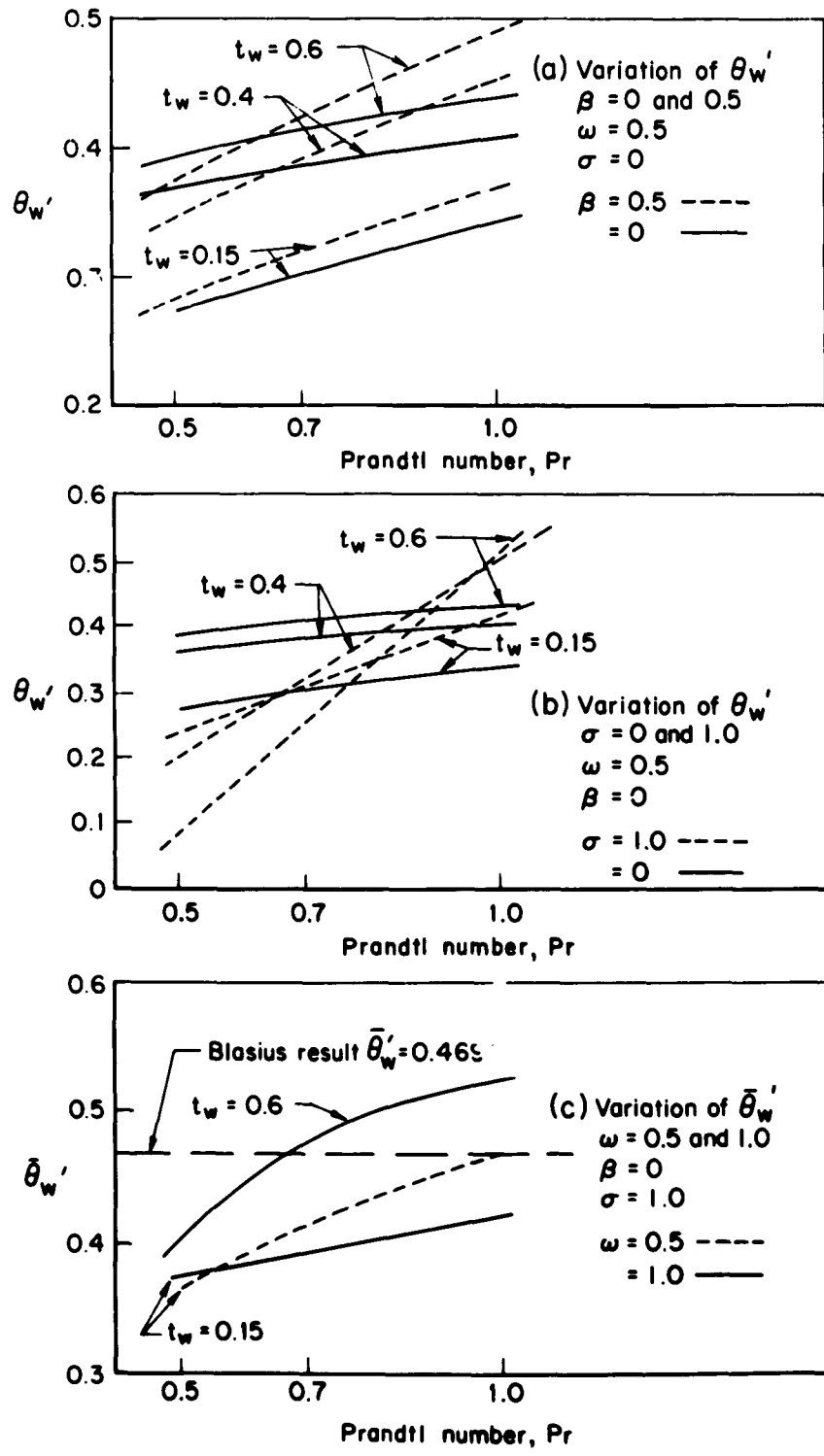


Fig. 10---Effects of Prandtl number on heat transfer

Equation (14) becomes somewhat inaccurate for values of $f_w < -0.6$ and $\beta > 0.5$, but for moderate values of these parameters the predicted value of t_{aw} is correct to better than 1 per cent. From Eq. (14) and (b) of Fig. 10, the important effects of Prandtl number on surface heat transfer may be seen. The familiar Blasius value $\theta_w' = 0.4696$ for a flat plate with $Pr = \omega = 1$ may overestimate the surface heat transfer in hypersonic flow by a factor of 2 or more, even for a moderately cooled wall.

The normalized enthalpy gradient $\bar{\theta}_w'$ shows a much smaller change with Prandtl number than the gradient θ_w' . It is indicated in (c) of Fig. 10 that the normalized derivative $\bar{\theta}_w'$ is close to the classical Blasius value even in hypersonic flow. From Figs. 3, 4, 5, and 10, it may be concluded that classical value $\bar{\theta}_w' = 0.4696$ is a good approximation over large ranges of Prandtl number, viscosity parameter, pressure-gradient parameter, and wall temperature. Combining this result with Eq. (14), the enthalpy derivative θ_w' may be determined.

V. EFFECTS OF LARGE INJECTION

Early theoretical calculations for mass transfer into a laminar boundary layer on a flat plate^(7,8) indicated the existence of "blow-off" points, i.e., separation of the boundary layer, at high mass-injection rates. These points were determined by noting the values of $f_w'' = \frac{\rho_w v_w}{\rho_e u_e} \sqrt{(Re_x)}$ for which $f_w'' \sim \left(\frac{du}{dy_w}\right) = 0$. Early efforts to correlate the exact solutions for the laminar boundary layer on a flat plate with mass transfer (see, e.g., Gross, et al.,⁽⁹⁾) suggested the use of a linear relationship between the mass-injection parameters f_w and the dimensionless skin friction:

$$\frac{c_f}{c_{f_0}} = 1 - 2.08 \left\{ \frac{\rho_w u_w}{\rho_e u_e} \sqrt{\frac{Re_x}{C^*}} \right\}, \quad (15)$$

where

c_f = local skin friction with mass transfer

c_{f_0} = local skin friction without mass transfer.

Extrapolation of this result would give an $f_w \approx -0.5$ for the blowoff point where $c_f = 0$. Hartnett and Eckert,⁽¹⁰⁾ Scott,⁽⁸⁾ and Hayday⁽¹¹⁾ showed that a similar blowoff point was not evident in the case of stagnation-point flows. In Gross, et al.,⁽⁹⁾ a comparison is made between flat-plate, wedge, and stagnation-point flows to show the effects of pressure gradient on the dimensionless heat transfer θ_w' . The implication was that a blowoff point for stagnation flows--if it existed--would occur at a much greater value of f_w than for the flat plate.

In this study, calculations were carried out to determine the behavior of the velocity gradient and the enthalpy gradient at the wall for a stagnation-point boundary layer for large values of the blowing parameter $|f_w|$. The results shown in Fig. 11 indicate that the solutions are asymptotic and that a blowoff point is never achieved, even though the values of the enthalpy gradient become quite small. It seems clear from the calculations that f_w'' will approach zero only at

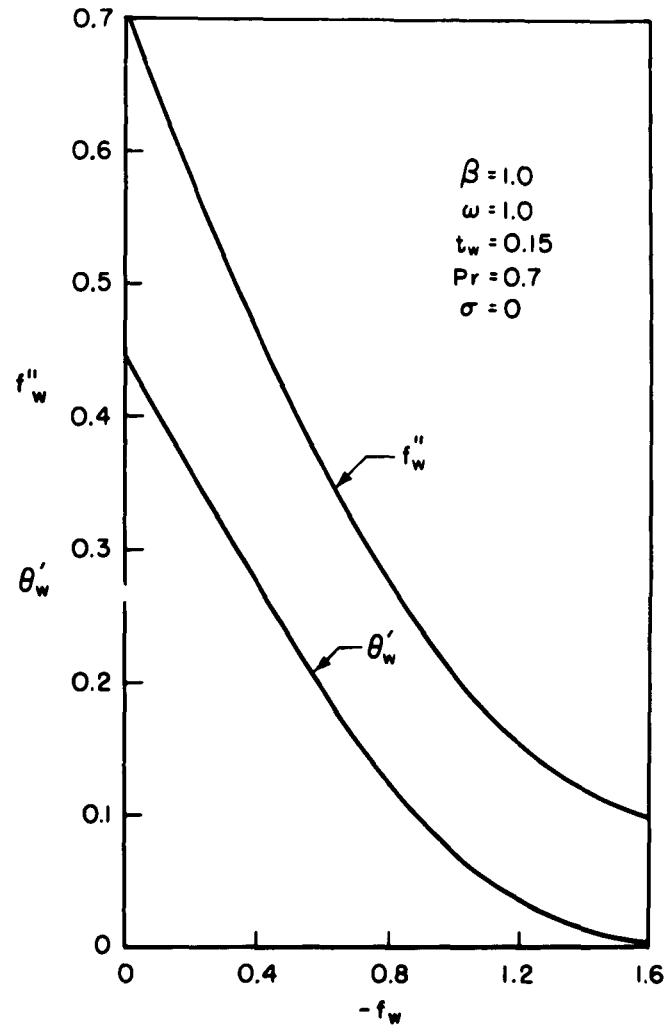


Fig. 11---Wall velocity gradient and heat transfer with large injection: two-dimensional stagnation point

very large values of $-f_w$. Figures 12 and 13 show the development of the profiles for the velocity and enthalpy and their gradients for increasing values of the mass-transfer parameter $|f_w|$. The solid-wall profiles have been included for comparison. It is interesting to note the drastic effect of the mass-transfer parameter in shifting the peak enthalpy toward the outer edge of the boundary layer. The increase in the thickness of the boundary layer with mass injection is graphically illustrated in these figures.

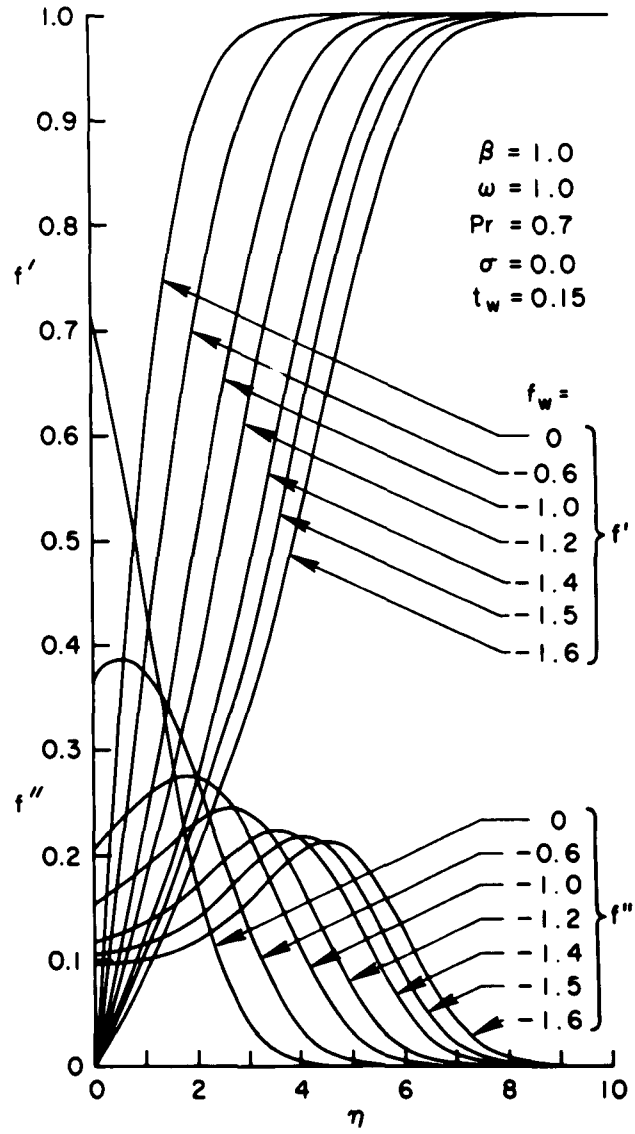


Fig. 12---Velocity and velocity-gradient distributions with injection

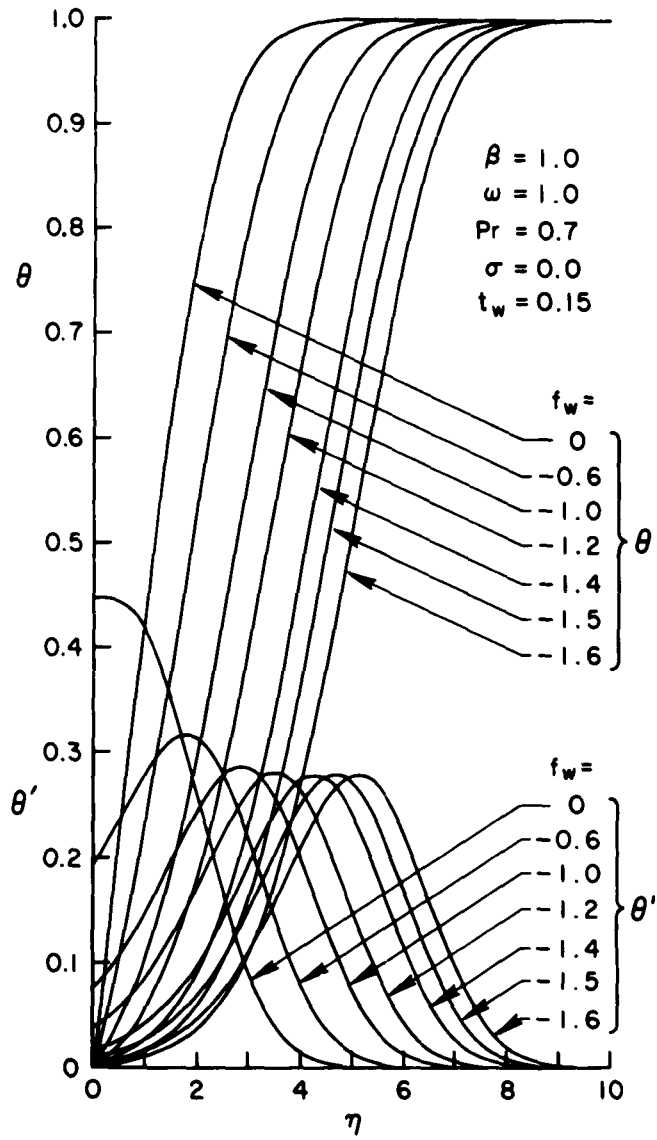


Fig. 13---Enthalpy and enthalpy-gradient distributions with injection

VI. BEHAVIOR OF THE BOUNDARY LAYER IN THE HYPERSONIC LIMIT

The influence of the hypersonic parameter $\sigma = (u_\infty^2/2H_e)(u_e/u_\infty)^2$ on the wall shear f'_w , the normalized enthalpy gradient $\bar{\theta}'_w$, and the displacement-thickness integral I_1 is considered in Figs. 14 and 15. The ordinate is given in terms of the ratios

$$\frac{f'_w}{(f'_w)_{\sigma=1}}, \quad \frac{\bar{\theta}'_w}{(\bar{\theta}'_w)_{\sigma=1}}, \quad \frac{I_1}{(I_1)_{\sigma=1}},$$

where the subscript $\sigma = 1$ indicates a value for the hypersonic limit $\sigma \rightarrow 1$ [$T_e/T_o \rightarrow 0$]. The integral I_1 is related to the displacement thickness δ^* by the equations⁽¹⁾

$$\delta^* = \frac{(25)^{1/2}}{\rho_w u_e} \frac{T_o}{T_e} \left[I_1 - \left(\frac{T_e}{T_o} \right) I_2 \right]; \quad (16)$$

$$I_1 = \int_0^\infty \left[(1 - f'^2) - (1 - t_w)(1 - \theta) \right] d\eta; \quad (17)$$

$$I_2 = \int_0^\infty f'(1 - f') d\eta. \quad (18)$$

For the hypersonic boundary layer, $(T_o/T_e) \approx \left(\frac{\gamma - 1}{2} \right) M_e^2 \gg 1$, and δ^* is very nearly proportional to the product $M_e^2 I_1$.

The ratios of f'_w , $\bar{\theta}'_w$, and I_1 increase with increasing values of σ . The maximum change in the ratios is about 20 per cent between $\sigma = 0$ and $\sigma = 1$. One important conclusion may be immediately drawn: The similarity requirement that the ratio $(u_e/u_\infty)^2$ be constant along the body surface is not a severe restriction, since large changes in this quantity (i.e., in σ) do not have a proportionately large effect on the boundary-layer solutions.

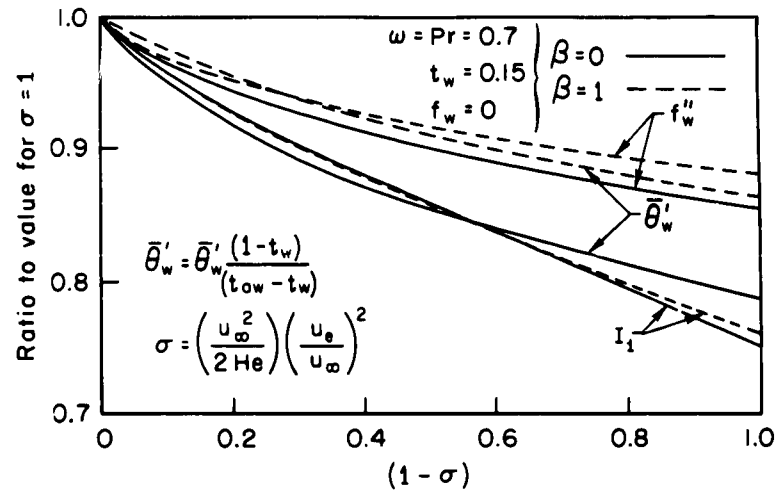


Fig. 14---Influence of hypersonic parameter σ on skin friction, heat transfer, and displacement thickness: $t_w = 0.15$

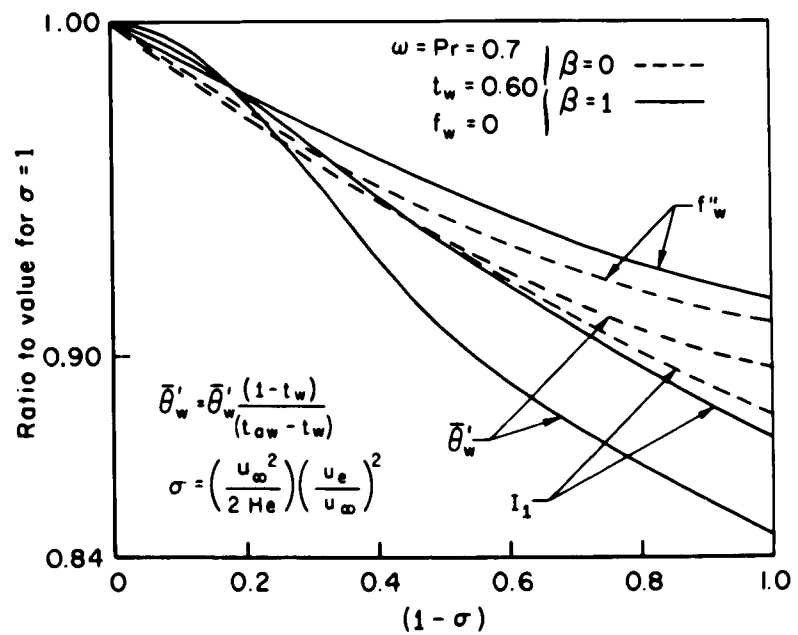


Fig. 15---Influence of hypersonic parameter σ on skin friction, heat transfer, and displacement thickness: $t_w = 0.60$

The change in f'_w , $\bar{\theta}'_w$, and I_1 with σ is nearly independent of β . A comparison of Figs. 14 and 15 shows that the ratios suffer a larger change with a lower wall temperature. From Eq. (14), and Figs. 14 and 15, it may be deduced that the enthalpy derivative θ'_w decreases with increasing σ , and the variation is greater with increasing wall temperature.

VII. CONCLUDING REMARKS

The results of this study may be succinctly stated as follows:

1. The effect of changing ω in the power-law viscosity $\mu \propto T^\omega$ on the enthalpy and velocity profiles is most important for low wall temperatures. Differences of 20 - 30 per cent in predicted heat transfer and skin friction for $0.5 \leq \omega \leq 1$ are observed at $t_w = 0.15$.

2. The effect of varying the Prandtl number on the enthalpy distribution in the boundary layer is important for low wall temperature ($t_w \approx 0.15$) and large values of the hypersonic parameter σ .

3. The laminar boundary layer at a stagnation point for a cold wall does not "blow off" or separate even at high blowing rates. Calculations indicate that $\theta'_w \rightarrow 0$ much more rapidly than f''_w , and that for $f'_w < -1.2$, $\theta'_w \approx 0$, while f''_w is finite.

4. The numerical solutions show that the viscous-dissipation term* has, at most, a 10 - 20 per cent effect on the wall shear f''_w , the displacement thickness I_1 , and the normalized enthalpy gradient $\bar{\theta}'_w$; these three quantities reach a maximum value for $\sigma \rightarrow 1$, i.e., in the hypersonic limit.

5. If the enthalpy gradient θ'_w is normalized to $\bar{\theta}'_w$ where

$$\bar{\theta}'_w = \theta'_w \frac{(1 - t_w)}{(t_{aw} - t_w)},$$

then the function $\bar{\theta}'_w$ is only weakly dependent upon the Sutherland constant s . In general, $\bar{\theta}'_w$ increases with both wall temperature t_w and pressure-gradient parameter β .

6. The boundary-layer characteristics calculated using a Sutherland-law viscosity can be approximated almost exactly using a power-law viscosity $\mu \propto T^{\omega_r}$ if the ω_r is determined empirically from the equation

*Third term on left side of Eq. (2).

$$\psi_r = \frac{3}{2} + \frac{\ln\left(\frac{t_w + s}{t_r + s}\right)}{\ln\left(\frac{t_r}{t_w}\right)},$$

where t_r is the Eckert reference temperature, and s is a temperature constant for the gas.

REFERENCES

1. Dewey, C. F., Jr., "Use of Local Similarity Concepts in Hypersonic Viscous Interaction Problems," AIAA J., Vol. 1, 1963, pp. 20-33.
2. Beckwith, I. E., Similar Solutions for the Compressible Boundary Layer on a Yawed Cylinder with Transpiration Cooling, NASA TR-R-42, 1959 (supersedes NACA TN-4345, 1958); see also E. Keshotko, and J. E. Beckwith, Compressible Laminar Boundary Layer over a Yawed Infinite Cylinder with Heat Transfer and Arbitrary Prandtl Number, NACA Report 1379, 1958 (supersedes NACA TN 3986, 1957).
3. Van Driest, E. R., Investigation of the Laminar Boundary Layer in Compressible Fluids using the Crocco Method, NACA TN 2597, 1952.
4. Cohen, C. B., and E. Reshotko, Boundary Layer with Heat Transfer and Pressure Gradient, NACA Report 1293, 1956 (supersedes NACA TN 3325, 1955).
5. Rubesin, M. W., and H. A. Johnson, "A Critical Review of Skin-Friction and Heat-Transfer Solutions of the Laminar Boundary Layer of a Flat Plate," Trans. ASME, Vol. 71, 1999, pp. 383-388.
6. Eckert, E.R.G., "Engineering Relations for Heat Transfer and Friction in High-Velocity Laminar and Turbulent Boundary-Layer Flow over Surfaces with Constant Pressure and Temperature," Trans. ASME, Vol. 56, 1956, pp. 1273-1283.
7. Gross, J. F., Skin Friction and Stability of a Laminar Binary Boundary Layer on a Flat Plate, The RAND Corporation, RM-3485-PR, January 1963.
8. Scott, C. J., The Application of Constant Property Solutions to Mass Transfer Cooling Calculations, Rosemount Aeronautical Laboratories, University of Minnesota, Engineering Memorandum No. 76, December 1958.
9. Gross, J. F., J. P. Hartnett, D. J. Masson, and Carl Gazley, Jr., "A Review of Binary Boundary Layer Characteristics," Int. J. Heat and Mass Transfer, Vol. 3, No. 3, 1961, pp. 198-221.
10. Hartnett, J. P., and E. R. G. Eckert, Mass Transfer Cooling in a Laminar Boundary Layer with Constant Fluid Properties, University of Minnesota Heat Transfer Laboratory Technical Report No. 4, 1955.
11. Hayday, A. A., Mass Transfer Cooling in a Laminar Boundary Layer in Steady Two-Dimensional Stagnation Flow, University of Minnesota Heat Transfer Laboratory TN 19, April 1958.